ZIBELINE INTERNATIONAL™ PUBLISHING

ISSN: 2523-5664 (Print)
ISSN: 2523-5672 (Online)
CODEN: WCMABD

Water Conservation & Management (WCM)

DOI: http://doi.org/10.26480/wcm.02.2021.92.96

RESEARCH ARTICLE

OPTIMIZATION AND CHARACTERIZATION OF CALCINATED CHICKEN EGG SHELL DOPED TITANIUM DIOXIDE PHOTOCATALYST BASED NANOPARTICLES FOR WASTEWATER TREATMENT

Yigezu Mekonnen Bayisa, Tafere Aga Bullo, Mohammed Seid Bultum

School of Chemical Engineering, Jimma Institute of Technology, Jimma University, Jimma, Oromia, Ethiopia.
**Corresponding author email: yigezu338@gmail.com*

ARTICLE DETAILS

Article History:

Received 18 September 2021
Accepted 20 October 2021
Available online 26 October 2021

ABSTRACT

In recent decades, research concerning and knowledge about the external benefits of renewable raw materials have intensified the efforts for investigating the major sources, causes, and effects of wastewater from solid waste and industries or households. In this study bio-matter and low-cost photocatalyst was prepared for photodegradation on the removal of methylene blue from wastewater treatment, and characterized by Fourier-transform infrared (FTIR) spectroscopy, UV-spectrometer, and X-ray diffractometer (XRD). The effects of initial concentration of methylene blue, amount of dopant, and degradation time were investigated on the percentage degradation of methylene blue using the calcinated eggshell doped titanium dioxide *nanoparticle* catalysts. At sufficient contact time and low initial concentration, the increment in dopant dose from 0.5 to 2.5 g/l results in an increment of methylene blue degradation efficiency, from 52.5 % to 95.8%. It was shown that a calcinating eggshell doped titanium dioxide photocatalyst method for wastewater treatment is a promising option for the degradation of methylene blue from industrial wastewater under the stated condition.

KEYWORDS

Calcinating Eggshell, Calcinating Eggshell Doped Titanium Dioxide, Photocatalyst, Wastewater Treatment

1. INTRODUCTION

Now a day the health problem connected with water pollution is the major and primary issue throughout the world (Raizada et al., 2020). Thus, the main cause of water pollution is, directly and indirectly, related to human activities that lead to the poor control of wastewater. The focal sources of wastewater is derived from a weak controlling mechanism of wastes from the industry plus from humans, animals, household, laundry and faesal sludge might be due to the lack of treatment services, or the fact that the existing facilities are not functioning as intended (Review et al., 2020). Usage of this untreated wastewater in agricultural activities are led to risk for both farmers in contact with water and crop consumers through transfer of pathogenic organisms (microbes that cause disease) from water to crop. Using this untreated wastewater causes waterborne diseases that can be transmitted through drinking water which contains the pathogen are, cholera, typhoid fever, diarrhea, and dysentery (Nanomaterials, 2021).

While quick industrial expansion is considered as an indicator of economic improvement, in other cases, they are greatly associated with environmental degradation, mainly due to the discharge of untreated wastewater or partially treated wastewater (Alani et al., 2021; Amin et al., 2018). In addition to this, most of the industries discharge their wastewater to near around water stream without adequate treatment, due to the lack of know-how and financial support. Therefore, effort should be made towards providing a wastewater treatment option for these industries to allow environmentally friendly disposal of their wastewater that reaches specific effluent quality goals.

The industrial expansion coupled with a weak controlling mechanism of wastewater from the industry plus humans, animals, household, laundry, and toilet in the country has led to extensive leads to environmental pollution (Shahmoradi et al., 2019). Due to low-profit margins, many industries failed to afford investment costs in pollution remediation equipment and technologies (Kumar et al., 2017). Those who have better capital are not willing to install efficient treatment technologies, due to lack of governmental control and weak implementation of environmental policies in the country (Ngoepe et al., 2020). There are several available methods for the exploitation and purification of wastewater, particularly photocatalytic activity of doped titanium dioxide (TiO_2) purposely removal of contaminants from wastewater (Mustapha et al., 2020; Dong et al., 2015). Titanium dioxide is the most common photocatalytic with the best performance, low price, and toxicity.

Titanium dioxide is a quite versatile technology that can be applied in many different situations and capable of handling many different forms and amounts of organic waste (Banerjee et al., 2018). From its behavior, TiO_2 can absorb only UV light, and UV light is just a small part of solar energy. There are different metal or nonmetal ion-doped with TiO_2 such as B, C, N, Fe^{3+}, CO_3^{-}, and Zn^{2+} the used to increase light absorption of TiO2 from UV to the visible range (Al-Mamun et al., 2019). When TiO_2 is coupled with CO_3^{-} ion as a catalyst which improves the capability of the oxidation photocatalyst reactions activity is faster that makes it very good-looking

Quick Response Code	Access this article online	
	Website: www.watconman.org	DOI: 10.26480/wcm.02.2021.92.96

Cite The Article: Yigezu Mekonnen Bayisa, Tafere Aga Bullo, Mohammed Seid Bultum (2021). Optimization and Characterization of Calcinated Chicken Egg Shell Doped Titanium Dioxide Photocatalyst Based Nanoparticles For Wastewater Treatment. *Water Conservation & Management, 5(2): 92-96.*

and increases the light absorption band energy of TiO_2 and increases the photocatalytic activity of TiO_2 under visible light irradiation (Yang et al., 2018; Amarasinghe and Wanniarachchi, 2019). Therefore, this CO_3^- can be drive from different biomass containing $CaCO_3$ specifically from chicken eggshell waste. Besides this, TiO_2-$CaCO_3$ can be created through the surface hydroxyl group in the liquid phase system at the interface of a phase of $CaCO_3$ and TiO_2 since CO_3^- is generated in-situ on the catalyst surface (Amarasinghe and Wanniarachchi, 2019).

Poultry eggs biomass, eggshells contain 94–97 wt.% $CaCO_3$, due to its randomized porous structure, locally available, waste resources, eco-friendliness, low cost, and nontoxicity can be used as a carrier for nano-biomass. Synthesizing calcinated chicken eggshell doped TiO_2 photocatalysts with a porous structure generate CO_3^- species for methylene blue degradation under light illumination (Huang et al., 2021; Echabbi et al., 2019). In the present study, low-cost photocatalyst was synthesized by calcinated chicken eggshell doped TiO_2 photocatalysts a sol-gel method for the degradation of methylene blue under solar light irradiation. The possible degradation pathway and the photocatalytic mechanism of methylene blue degradation over calcinated chicken eggshell is determined. Response surface methodology (RSM) is applied to optimize the reaction conditions and further evaluate the interaction among the selected process parameters.

2. Materials and Methods

2.1 Materials and Reagents

The photocatalyst employed was commercial 98% titanium dioxide (TiO_2) produced by Loba Chemie Pvt. Ltd in India was purchased from Atomic Educational Materials Supply PLC in Addis Ababa. The methylene blue powder and Copper sulfate granular ($CuSO_4.5H_2O$) were provided by Jimma University, Department of Chemistry.

2.2 Synthesis of Calcined Egg Shells (CES)

Chicken eggshells were collected from different Jimma Institute of Technology staff launches and soaked in hot water for 5-10min and washed with tap water repeatedly to remove different impurities. The shells were dried in an oven at 105 °C for 12 h. Finally, the dried shells were crushed to a uniform size by selecting the powder using a sieve of 200mesh. The crushed eggshell powder was put into an alumina crucible and calcined in a muffle furnace at 1000°C temperatures for $1\frac{1}{2}$ hr. The obtained material was washed with distilled water, dried overnight at 105°C, and then calcined at a rate of 2 °C/min until reaching 400 °C. It was maintained at this temperature for 4 h. The resulting material was stored in a glass bottle for use without any pretreatment and is called Calcined Egg Shells (CES).

2.3 Preparation of CES doped TiO_2

The equal proportion mixture of TiO_2 and CES was introduced into a vessel equipped with a stirrer. The homogenization of the two mixtures was carried out by adding a small amount of distilled water. The solution was concentrated by removing the water and heated in the oven at 105°C for 12 h, and the sample was dried. The homogenized fine powder material was obtained and calcined at 400 °C for 4 h (Echabbi et al., 2019). The obtained powder was washed with distilled water, dried, and characterized.

2.4 Characterization of CES doped TiO_2 photocatalyst

TiO_2 and CES doped TiO_2 catalysts were characterized by using an X-ray diffractometer (XRD-7000) and a Fourier Transform Infrared (FTIR) spectroscopy Nicolet model Protégé 460 Magna IR spectrometer. The X-ray diffractometer was used to show that the samples crystalline structure and to identify the presence of anatase, rutile, and brookite phase. FTIR spectroscopy was used to identify functional groups of organic and inorganic compounds present in the photocatalyst.

2.4.1 FTIR Analysis

The FTIR spectrum of the photocatalysts was obtained using PerkinElmer Spectrum and the functional groups were determined with the help of IR correlation charts. The wavenumber region for the analysis was 4000-400 cm^{-1}.

2.4.2 XRD Analysis

The XRD analysis for the crystal structure of the photocatalysts was obtained using a Darwell XRD 7000, with Kα (3kW) x-ray diffractometer. The analysis was conducted in a range of 10-90^0 at a scanning speed of 0.0300 ^{0}C/sec.

2.4.3 UV-vis Spectroscopy analysis

The UV-vis spectroscopy analysis for identifying the maximum wavelength was obtained using Specord 200 Plus UV-vis spectroscopy. The maximum wavelength was obtained by dissolving photocatalysts in ethanol and using a water-ethanol mixture as a baseline. Then, those wavelengths were used to calculate the band gap of both photocatalysts.

2.5 Photocatalytic degradation of Methylene Blue

The photocatalytic activity was accomplished using dye (Methylene blue) from industrial effluents that were treated under a 9W LED lamp at a distance of 10 cm. Then the synthesized CES doped TiO_2 has added to Methylene blue solution in a reactor equipped with a magnetic stirrer, pH meter, a thermometer, and a water bath. After the treatment, desorption of the pollutants from the surface of the catalyst was accomplished by modification of the solution pH. The catalyst was removed by centrifugation (3500 rpm).

2.5.1 Experimental design

Response Surface Methodology was used to determine the effects of photodegradation on the removal of methylene blue. A BBD with three numerical factors on three levels was used. They consisted of 15 randomized runs. A concentration of methylene blue, 100 to 300 ppm, amount of dopant, 0.08 to 0.4 %, and degradation time were investigated as independent variables. The responses (Y), presented as percentage degradation of methylene blue using the catalysts that were synthesized under the above conditions, calculated from an initial (C_0, ppm) and residual methylene blue concentrations (C_t, ppm) at sampling time t, degradation efficiencies were measured by the following formula.

$$Degradation\ efficiency, Y\ (\%) = \frac{C_{MBO} - C_{MB}}{C_{MBO}} * 100$$

Where, C_MBO is the initial concentration of MB and C_MB is the concentration of MB at the time of sampling.

3. Results and Discussion

3.1 Analysis of photocatalyst

The photocatalyst of CES doped titanium dioxide was characterized by FT-IR, XRD, and UV-vis Spectroscopy analysis for determination of their functional group, structure, and bandgap energy respectively. There result is shown in Figures 1 to 3. As it is shown in figure 1a the highest peak is at 3500 $cm^{-1}$and the lowest peak is around 3125 cm^{-1} which shows that they are both in the single bond region. At wavenumber 3500 cm^{-1} there is an H bonded, and OH stretch bond which shows the existence of alcohol and phenols; while at 3125 cm^{-1} there is a C-H stretch bond that shows the existence of an aromatic ring. The peaks at 3625 cm^{-1} were attributed to alcohol and phenols since they show an O-H stretch and free hydroxyl bond (Amarasinge and Wanniarachchi, 2019; Khairy and Zakaria, 2014). The peaks around 680-610cm^{-1} show the presence of an $SO4^{2-}$ group.

The spectrum revealed the presence of a number of characteristic bands in the range of 400–4,000 cm^{-1} for pure CES as it shown in figure 1b. Broadband noticed from 3650-3120 cm^{-1} corresponds to hydroxyl functional group (OH stretching vibration), and maybe also the characteristic peak of carbonyl and hydroxyl groups, while the weak bands at 2920 cm^{-1} assigned to asymmetric C-H stretching. The bands observed in the region between 1700 cm^{-1} and 1490 cm^{-1} were attributed to C=C symmetrical stretching of pyrone groups and C=O of carboxylic groups. This may also be the band attributed as a result of amides groups and aromatic carbon-carbon stretching vibration. Moreover, the band observed at 1,632 cm^{-1} was assigned to carbonyl C–O present in carbonyls, ketones, aldehydes, or ester groups and C–C present in olefinic vibrations in the aromatic region[18]. The bands in the range of 1200-900 cm^{-1} have also been attributed to either Si-O or C-O stretching in alcohol, ether, or hydroxyl groups

The XRD analysis was conducted for both CES and CES doped TiO2 photocatalyst. XRD was used to confirm the formation of CES doped TiO2 nanoparticles prepared using MB water extract. The XRD pattern for both CES and CES doped TiO2 is shown in Figures 2a and b. The XRD pattern for pure CES has 6 peaks at 2θ=21.04O, 24.19O, 25.48O, 26.8O, 31.12O, and 50.26O. The major peak at 26.8O is attributed to anatase phase CES while

the peak at 50.26O shows the presence of the brookite phase (Echabbi et al., 2019). There was no rutile phase in the recorded peaks. The XRD pattern for the CES doped TiO2 has 6 peaks at 2θ=12.01 O, 21.19 O , 23.11O, 24.34 O, 25.57 O, 26.89 O, 28.21 O, 31.21O, and 50.32 O. The major peak at 26.89O is attributed to the presence of the anatase phase while the peak at 50.26O shows the presence of the brookite phase (Huang et al., 2021). The reason for the newly emerged peaks in the CES doped TiO2 is given to calcination the process of doping the photocatalyst.

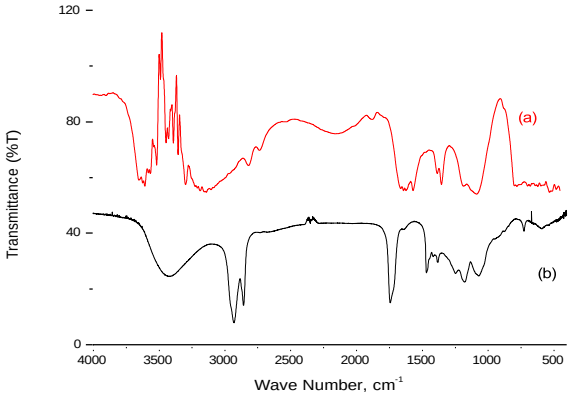

Figure 1: FTIR spectra of (a) CES doped TiO2 (b) pure CES

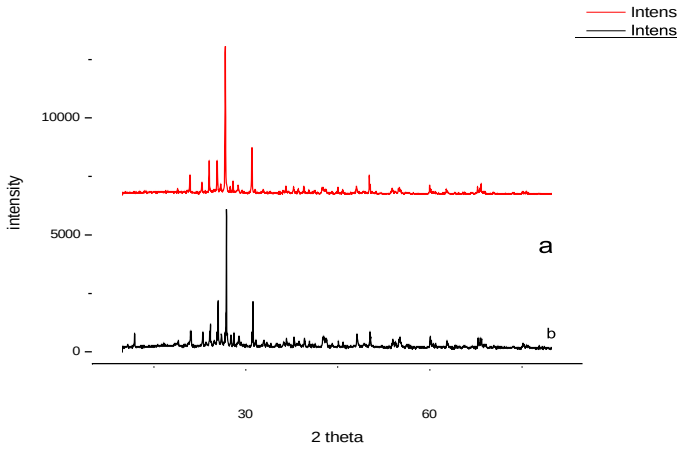

Figure 2: XRD patterns of a) CES b) CES doped Titanium oxide

Figure 3 reports the UV–vis absorbance spectra in terms of absorbance for TiO2 and CES doped TiO2. As it has shown from figure 3a the shifting of the absorption onset from about 303 nm (for undoped TiO2) to about 490 nm (for CES doped TiO2) indicates the ability of the sample to absorb visible light, as confirmed by the results in Figure 3b, which is the typical the observed optical band gap energy values indicate that CES doping results in a decrease of the unnecessary bandgap. Therefore, the band gap has lowered from 4.09 eV to 2.53 eV.

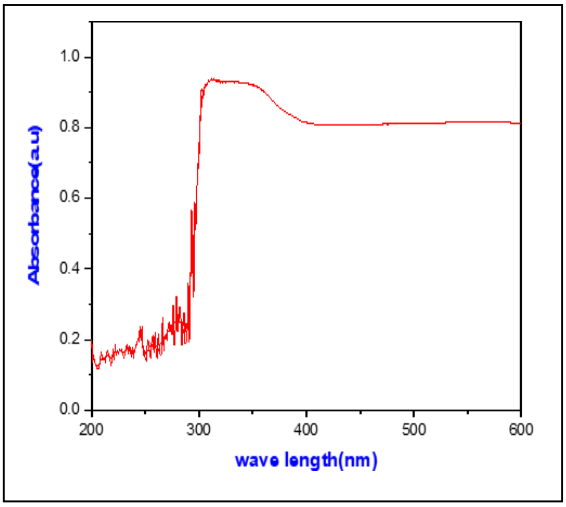

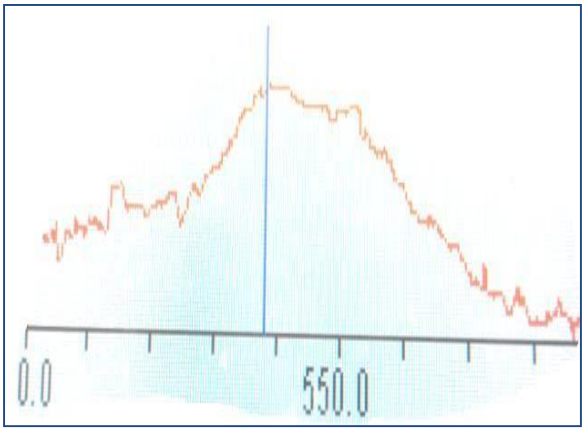

Figure 3: UV-Vis spectra of spectra of (a) TiO_2 pure (b) CES doped TiO_2

3.2 Photocatalytic Activity

3.2.1 Variables effect on the degradation efficiency of methylene blue

Based on the ANOVA analysis the parameter which significantly affected the degradation efficiency of methylene blue was shown in Table 1. From this table, the Model F-value of 331.86 implies the model is significant, P-values less than 0.0500 indicate model terms and all factors are significant and the Lack of Fit F-value of 1.47 implies the Lack of Fit is not significant.

Table 1: ANOVA analysis for process parameter

Sources	Sum of the squares	Sum of the mean	f-value	p-value	
Model	2161.92	240.21	331.86	<0.0001	significant
A-dosage of CES /TiO2	595.47	595.47	822.66	<0.0001	
B-concentration of MB	260.60	260.60	360.03	<0.0001	
C-degradation time	901.43	901.43	1245.35	<0.0001	
AB	0.0676	0.0676	0.0934	0.7722	
AC	0.1369	0.1369	0.1891	0.6818	
BC	84.09	84.09	116.17	0.0001	
Residual	3.62	0.7238			
Lack of Fit	2.49	0.8308	1.47	0.4285	Not significant

The response surface curves representing the parameter effects of three variables, i.e., a dosage of CES/TiO2, initial concentration of methylene blue, degradation or treatment time on methylene blue degradation compounds by CES/TiO2 photocatalyst were investigated.

Figure 4a shows that a maximum methylene blue degradation was attained at a high treatment time and a considerably low initial concentration of methylene blue. Increasing the photocatalyst dosage from 0.5 g/L to 2.5 g/L also increased the degradation efficiency. But, the later increase in degradation was smaller in range compared to the first showing that the effect of photocatalyst concentration on the degradation efficiency has slowed down. This is because increased amount of photocatalyst blocks the light from reaching some of the particles which makes some of the photocatalyst surfaces unavailable for light absorption, which is a sign that it has approached the optimum concentration of photocatalyst (Echabbi et al., 2019; Sen et al., 2018).

The initial concentration of methylene blue during the treatment process was significantly affecting the efficiency of photocatalytic degradation. As shown in figure 4a increasing the methylene blue concentration from 10 to 30 ppm the degradation efficiency of photocatalytic calcinated eggshell

doped with titanium dioxide was decreased i.e., a small amount of it can be adsorbed on the surface of the photo-catalyst, at higher concentration. On the other hand, a maximum methylene blue degradation was obtained at a relatively high dosage dopant and low initial concentration of methylene blue (Sohrabi and Akhlaghian, 2016; Xu et al., 2020). For instance, after three hours of UV irradiation, the degradation yields of methylene blue concentration at 10, 20, and 30 mg/L are about 95.8%, 84.8%, and 60.7%, respectively.

In this work efficiency of the photocatalytic calcinated eggshell, doped TiO_2 was significantly affected by contact time on adsorption of methylene blue degradation was presented in Figure 4b. As it can see in this figure the degradation efficiency of MB is directly proportional to the time spent in the degradation process. The sudden increase in degradation efficiency in the 180 minutes is attributed to the effect of the higher dopant concentration of photocatalyst. A higher concentration of photocatalyst has this effect because a higher concentration means it takes a longer time to react to start an efficient degradation process (Bind et al., 2018). And also due to the complex structure of the pollutant, methylene blue takes a longer time to reach and be degraded fully (Lazar et al., 2012). In general, at sufficient contact time and low initial concentration, the increment in dopant dose from 0.5 to 2.5 g/l results in an increment of methylene blue degradation efficiency, from 52.5 % to 95.8%.

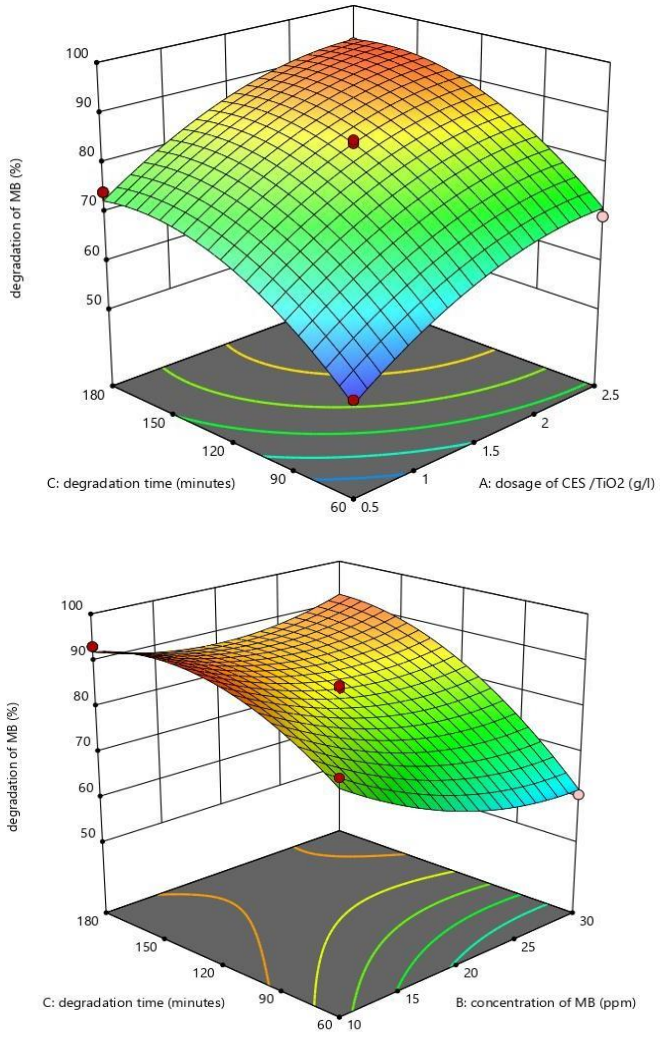

Figure 4: Effect of process parameter on the degradation efficiency of methylene blue

4.1.1 Optimization of methylene blue degradation efficiency

The program randomly picks a set of conditions from which to start its search for desirable results which was indicated as ramps function in figure 5. The Design-Expert then sorts the results from most desirable to least and as it shown from Figure 6. and 7, the predicted runs the optimum degradation efficiency of methylene blue was selected which is higher in desirability (0.863) than others which observed from constraints solution.

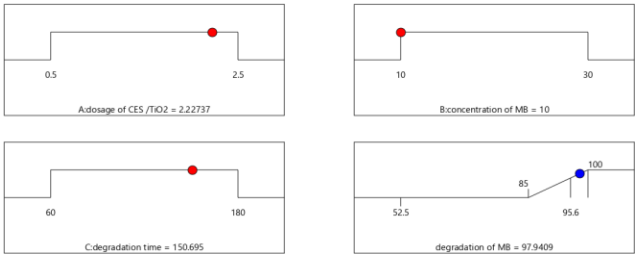

Figure 5: Optimization methylene blue degradation ramp's function

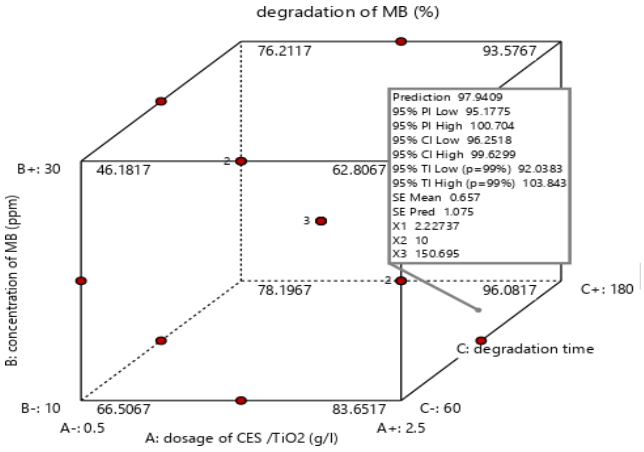

Figure 6: Optimization methylene blue degradation efficiency

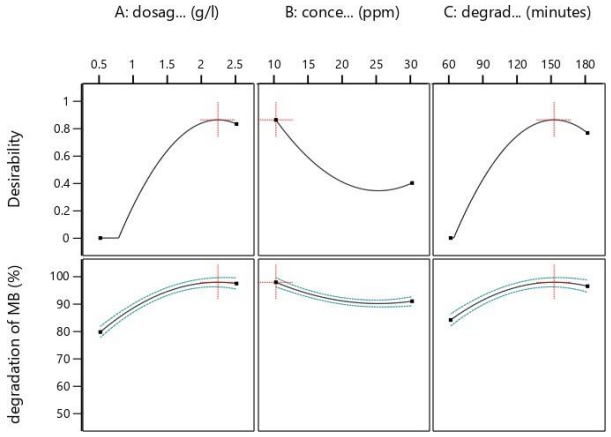

Figure 7: Constraint's solutions.

4. Conclusion

In this study CES doped titanium dioxide was investigated for degradation of methylene blue compound from industrial wastewater. The prepared CES doped titanium dioxide photocatalyst of functional group, structure, and bandgap energy was characterized by FT-IR, XRD, and UV-vis Spectroscopy analysis respectively. The result of the study shows that calcinated eggshell dopant is a good photocatalyst for degradation of methylene blue from wastewater decontamination due to the presence of potential binding sites and functional groups which confirm the degradation process. The prepared photocatalyst showed that 95.8% degradation efficiency of methylene blue was obtained at a contact time of 180 minutes, initial concentration of methylene blue of 10 ppm, and a dopant dose of 2.5 g/l. Therefore, the degradation process of methylene blue compounds using calcinated eggshell doped titanium dioxide photocatalyst from wastewater can be used as a useful treatment process.

Data Availability

Our data generated during the study are included in the manuscript.

Acknowledgments

We would like to acknowledge the XRD and FT-IR platform at the Faculty of Material Science and Engineering, Jimma University, for support in the FT-IR spectroscopy

Conflict of Interest

The authors declare that there is no conflict of interests regarding the publication of this article

Ethical Approval

This article does not contain any studies with human participants or animals performed by any of the authors.

Highlights

- Analysis of chicken eggshell wastes are being used as photocatalyst source to calcinated eggshell doped TiO_2, i.e., 'Waste to photocatalyst' for production of viable sustainable products to bio photocatalyst from waste to fulfill the need of an expensive metal-doped catalyst
- Photocatalytic degradation of Methylene Blue experiment has been done.

The highest degradation efficiency of 95.8 % methylene blue was obtained at a contact time of 180 minutes, 10 ppm of initial concentration of methylene blue, and a dopant dose of 2.5 g/l by using prepared photocatalyst.

References

Alani, O.A., Ari, H.A., Alani, S.O., Offiong, N.O., 2021. Visible-Light-Driven Bio-Templated Magnetic Copper Oxide Composite for Heterogeneous Photo-Fenton Degradation of Tetracycline.

Al-Mamun, M.R., Kader, S., Islam, M.S., Khan, M.Z.H., 2019. Photocatalytic activity improvement and application of UV-TiO2 photocatalysis in textile wastewater treatment: A review. J. Environ Chem Eng., 7 (5).

Amarasinghe, A., Wanniarachchi, D., 2019. Eco-Friendly photocatalyst derived from egg shell waste for dye degradation. J Chem.

Amin, F., Talpur, F.N., Balouch, A., Afridi, H.I., 2018. Efficient entrapping of toxic Pb (II) ions from aqueous system on a fixed-bed column of fungal biosorbent. Geol Ecol Landscapes [Internet], 9508 (Ii), Pp. 1–6. Available from: https://doi.org/10.1080/24749508.2018.1438746

Banerjee, S., Benjwal, P., Singh, M., Kar, K.K., 2018. Graphene oxide (rGO)-metal oxide (TiO2 /Fe3O4) based nanocomposites for the removal of methylene blue. Appl Surf. Sci., [Internet], 439, Pp. 560–8. Available from: https://doi.org/10.1016/j.apsusc.2018.01.085

Bind, A., Goswami, L., Prakash, V., 2018. Comparative analysis of floating and submerged macrophytes for heavy metal (copper, chromium, arsenic and lead) removal: sorbent preparation, characterization, regeneration and cost estimation. Geol Ecol Landscapes [Internet]. 9508, Pp. 1–12. https://doi.org/10.1080/24749508.2018.1452460

Dong, S., Feng, J., Fan, M., Pi, Y., Hu, L., Han, X., 2015. Recent developments in heterogeneous photocatalytic water treatment using visible light-responsive photocatalysts: A review. RSC Adv., 5 (19), Pp. 14610–30.

Echabbi, F., Hamlich, M., Harkati, S., Jouali, A., Tahiri, S., Lazar, S., 2019. Photocatalytic degradation of methylene blue by the use of titanium-doped Calcined Mussel Shells CMS/TiO2. J Environ Chem. Eng., 7 (5), Pp. 103293.

Hegazy, A.K., 2014. Adsorption of phenol onto activated carbon from Rhazya stricta: determination of the optimal experimental parameters using factorial design, Pp. 273–81.

Huang, Z., Wang, J., Yang, M.Q., Qian, Q., Liu, X.P., Xiao, L., 2021. Construction of tio2-eggshell for efficient degradation of tetracycline hydrochloride: Sunlight induced in-situ formation of carbonate radical. Materials (Basel), 14 (7).

Khairy, M., Zakaria, W., 2014. Effect of metal-doping of TiO2 nanoparticles on their photocatalytic activities toward removal of organic dyes. Egypt J Pet [Internet], 23 (4), Pp. 419–26. Available from: http://dx.doi.org/10.1016/j.ejpe.2014.09.010

Kumar, A., Balouch, A., Pathan, A.A., Muhammad, A., Jagirani, M.S., Mustafai, F.A., 2017. Remediation techniques applied for aqueous system contaminated by toxic Chromium and Nickel ion. Geol Ecol Landscapes [Internet], 9508, Pp. 1–11. Available from: http://doi.org/10.1080/24749508.2017.1332860

Lazar, M.A., Varghese, S., Nair, S.S., 2012. Photocatalytic water treatment by titanium dioxide: Recent updates, Catalysts., 2, Pp. 572–601.

Mustapha, S., Ndamitso, M.M., Abdulkareem, A.S., Tijani, J.O., Shuaib, D.T., Ajala, A.O., 2020. Application of TiO2 and ZnO nanoparticles immobilized on clay in wastewater treatment: a review [Internet]. Applied Water Science. Springer International Publishing., 10, Pp. 1–36. Available from: https://doi.org/10.1007/s13201-019-1138-y

Nanomaterials, C., 2021. Mechanism and Purification Effect of Photocatalytic Wastewater Treatment Using Graphene Oxide-Doped Titanium Dioxide.

Ngoepe, N.M., Mathipa, M.M., Hintsho-Mbita, N.C., 2020. Biosynthesis of titanium dioxide nanoparticles for the photodegradation of dyes and removal of bacteria. Optik (Stuttg) [Internet], 224 (June), Pp. 165728. Available from: https://doi.org/10.1016/j.ijleo.2020.165728

Raizada, P., Sudhaik, A., Patial, S., Hasija, V., Parwaz Khan, A.A., Singh, P., 2020. Engineering nanostructures of CuO-based photocatalysts for water treatment: Current progress and future challenges. Arab J. Chem., 13 (11), Pp. 8424–57. Available from: https://doi.org/10.1016/j.arabjc.2020.06.031

Review, W.A., Yaqoob, A.A., Parveen, T., Umar, K., 2020. Role of Nanomaterials in the Treatment of. Water., 12, Pp. 495.

Sen, B., Goswami, S., Devi, G., Sarma, H.P., 2018. Valorization of Adenanthera pavonina seeds as a potential biosorbent for lead and cadmium removal from single and binary contaminated system. Geol Ecol Landscapes [Internet]. 9508, Pp. 1–13. Available from: https://doi.org/10.1080/24749508.2018.1464266

Shahmoradi, B., Farahani, F., Kohzadi, S., Maleki, A., Pordel, M., Zandsalimi, Y., 2019. Application of cadmium-doped ZnO for the solar photocatalytic degradation of phenol. Water Sci Technol., 79 (2), Pp. 375–85.

Sohrabi, S., Akhlaghian, F., 2016. Modeling and optimization of phenol degradation over copper-doped titanium dioxide photocatalyst using response surface methodology. Process Saf Environ Prot [Internet], 99, Pp. 120–8. Available from: http://dx.doi.org/10.1016/j.psep.2015.10.016

Xu, Q., Wang, Y., Chi, M., Hu, W., Zhang, N., He, W., 2020. Porous polymer-titanium dioxide/copper composite with improved photocatalytic activity toward degradation of organic pollutants in wastewater: Fabrication and characterization as well as photocatalytic activity evaluation. Catalysts, 10 (3).

Yang, C.C., Doong, R.A., Chen, K.F., Chen, G.S., Tsai, Y.P., 2018. The photocatalytic degradation of methylene blue by green semiconductor films that is induced by irradiation by a light-emitting diode and visible light. J. Air. Waste. Manag. Assoc., [Internet]. 68 (1), Pp. 29–38. Available from: https://doi.org/10.1080/10962247.2017.1358222.